Acid Pairs Increase the N-Terminal Ca^{2+} Affinity of CaM by Increasing the Rate of Ca^{2+} Association[†,‡]

D. J. Black,*[,§] Svetlana B. Tikunova,[§] J. David Johnson,[§] and Jonathan P. Davis[||]

Department of Molecular and Cellular Biochemistry and Department of Physiology and Cell Biology, The Ohio State University Medical Center, Columbus, Ohio 43210

Received May 16, 2000; Revised Manuscript Received September 11, 2000

ABSTRACT: A series of N-terminal calmodulin (CaM) mutants was generated to probe the relationship between the N-terminal Ca^{2+} affinity and the number of paired, negatively charged Ca^{2+} chelating residues in the N-terminal Ca^{2+}-binding sites of CaM. When the number of acid pairs [negatively charged residues at positions $+x$ and $-x$ (*X*-axis), $+y$ and $-y$ (*Y*-axis), and $+z$ and $-z$ (*Z*-axis)] was increased from zero to one and then to two, a progressive increase was seen in the N-terminal Ca^{2+} affinities. The maximal ranges of the increases observed in the N-terminal Ca^{2+} affinity were ∼8−8.5-fold for site I, ∼4.5−5-fold for site II, and ∼11-fold for both sites, in comparison to the mutants containing no acid pairs. The maximal values of N-terminal Ca^{2+} affinity were bestowed by the presence of five acidic chelating residues in site I or II, individually. Addition of the sixth acidic chelating residue (third acid pair) to both N-terminal Ca^{2+}-binding sites reduced the N-terminal Ca^{2+} affinity. The increases in Ca^{2+} affinity observed were caused by an increase in the Ca^{2+} association rates for the *Y*- and *Z*-axis acid pairs, while the *X*-axis acid pair caused a reduction in the Ca^{2+} dissociation rates.

Calmodulin (CaM)[1] is a ubiquitous Ca^{2+}-binding protein that binds two Ca^{2+} ions in each of its N- and C-terminal globular domains. Binding of Ca^{2+} allows CaM to bind and regulate multiple target enzymes (for a review, see ref *1*). The Ca^{2+} binding properties of CaM have been studied extensively both statically and kinetically and under numerous environmental conditions (variable temperatures, ionic strengths, pHs, and concentrations) (*2*−*7*), making it an excellent model for determining the fundamental structural elements essential for ion binding and specificity in Ca^{2+}-binding proteins (*8*−*10*). The basic protein motif that allows CaM, and numerous other Ca^{2+}-binding proteins, to bind Ca^{2+} is the EF-hand.

The EF-hand consists of a helix−loop−helix secondary structure elucidated from the crystal structure of carp parvalbumin (*11*). Most EF-hand Ca^{2+}-binding proteins contain coupled EF-hands that bind Ca^{2+} in a concerted manner (*12*, *13*). A canonical EF-hand is comprised of 29 consecutive amino acids with the first nine forming an

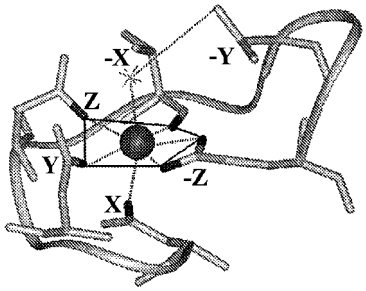

	X	*	Y	*	Z	*	-Y	*	-X	*	*	-Z
Loop 1:	D		D		D		T		T			E
Loop 2:	D		D		N		T		D			E

FIGURE 1: Ca^{2+} coordination by Ca^{2+}-binding site I of calmodulin. Ca^{2+}-binding site I of calmodulin is used to illustrate the pentagonal bipyramidal coordination of Ca^{2+}. The chelating oxygen atoms of the coordinating residues are colored black and are shown to interact with the spherical Ca^{2+} ion via the dashed lines. The coordinating oxygen atoms that form the base of the pentagonal bipyramid are connected with the solid black lines. This figure was made by Melanie R. Nelson, in Walter J. Chazin's laboratory at the Scripps Research Institute. The molecular model was produced in InsightII (MSI, San Diego, CA). This is a modified version of a figure that appeared in the chapter Calmodulin as a Calcium Sensor in *Calmodulin and Signal Transduction* (by M. R. Nelson and W. J. Chazin, pp 17−64). Below are the residues in the *X*, *Y*, and *Z* positions in Ca^{2+}-binding sites I and II.

α-helix, followed by a 12-residue loop with the last three residues beginning another 11-residue α-helix. The loop domain of the EF-hand contains six chelating residues that coordinate the Ca^{2+} ion through seven oxygen atoms. These residues are denoted by their position in the linear sequence of the 12-amino acid loop and by the tertiary geometry imposed on the residues which align on the axes of a pentagonal bipyramid as follows (see Figure 1): positions 1 ($+x$), 3 ($+y$), 5 ($+z$), 7 ($-y$), 9 ($-x$), and 12 ($-z$). The *Y*-

† This research was funded, in part, by NIH Grant DK33727.

‡ In memory of J. David Johnson, mentor and friend.

* To whom correspondence should be addressed: Department of Cellular and Molecular Biochemistry, The Ohio State University Medical Center, 363 Hamilton Hall, 1645 Neil Ave., Columbus, OH 43210. Telephone: (614) 292-0104. Fax: (614) 292-4118. E-mail: black.215@osu.edu.

§ Department of Molecular and Cellular Biochemistry.

|| Department of Physiology and Cell Biology.

[1] Abbreviations: CaM, calmodulin; sTnC, skeletal troponin C; Hepes, *N*-(2-hydroxyethyl)piperazine-*N*′-2 ethanesulfonic acid; MOPS, 4-morpholinepropanesulfonic acid; EGTA, ethylene glycol bis(β-aminoethyl ether)-*N*,*N*,*N*′,*N*′-tetraacetic acid; W, CaM mutant with the Phe19Tryp mutation; I and II, Ca^{2+}-binding loops in the first and second N-terminal EF-hands of CaM, respectively; *X*, *Y*, and *Z*, acid pairs that are present in each Ca^{2+}-binding loop.

10.1021/bi001106+ CCC: $19.00
Published on Web 10/14/2000

and *Z*-axis acid pairs align along the vertexes of an approximately planar pentagon, with the *X*-axis acid pair having an orientation that is perpendicular to the *Y*- and *Z*-axis plane (for a review, see ref *14*).

Multiple structural factors govern the Ca^{2+} affinity in EF-hand proteins. These include the hydrophobicity of flanking helices and the loop itself (*10*, *15*−*18*), nonchelating residues within the loop (*10*, *19*), and the number and location of charged residues within the loop at chelating positions (*10*, *20*−*23*). Reid and Hodges put forth the acid pair hypothesis that related the location of negatively charged residues at chelating positions to Ca^{2+} affinity (*24*). This hypothesis predicts the highest Ca^{2+} affinity will occur in a single EF-hand when there are a maximum of four acidic residues in chelating positions 1, 5, 9, and 12 causing pairing of the carboxylate oxygen atoms at the $+x$ and $-x$ (*X*-axis) and $+z$ and $-z$ (*Z*-axis) positions. It further states that introduction of a fifth carboxylate chelating residue should decrease the Ca^{2+} affinity due to an increased level of electrostatic repulsion. Synthetic EF-hand peptide fragments based on the third Ca^{2+}-binding sites of skeletal troponin C (sTnC) and CaM originally showed the validity of the acid pair hypothesis (*25*−*27*). The hypothesis held true in the third Ca^{2+}-binding site of CaM when the fourth Ca^{2+}-binding site's ability to bind Ca^{2+} was eliminated by another mutation (*9*).

To test the role of increasing the number of acid pairs in a functional, coupled EF-hand protein system, we increased the number of acid pairs in N-terminal Ca^{2+}-binding sites of CaM from zero to three by mutating the chelating residues that have the highest variability within the known EF-hands, the z, $-y$, and $-x$ positions, to Asp. We found that the native acid pairs in the N-terminus of CaM, *Z*-axis in site I and *X*-axis in site II, are responsible for an ~4.6 and 2.5-fold increase in the N-terminal Ca^{2+} affinity in relation to the mutant CaM without an acid pair in one N-terminal Ca^{2+}-binding site and the other unmodified N-terminal Ca^{2+}-binding site, respectively. Often, a subsequent addition of an acid pair at any location further increased the N-terminal Ca^{2+} affinity in the mutant CaMs. The endogenous acid pairs from both N-terminal Ca^{2+}-binding sites of CaM are responsible for an approximate 11-fold increase in N-terminal Ca^{2+} affinity relative to a mutant CaM lacking acid pairs. Completely filling the acid pairs in the N-terminal Ca^{2+}-binding sites of CaM caused only an ~2-fold increase in N-terminal Ca^{2+} affinity compared to that of a mutant CaM lacking acid pairs. The observed alterations in N-terminal Ca^{2+} affinity can be explained primarily by changes in the Ca^{2+} association rates mitigated by alterations in the Ca^{2+} dissociation rates.

EXPERIMENTAL PROCEDURES

Materials. The phenyl-Sepharose CL-4B and EGTA were purchased from Sigma Chemical Co. (St. Louis, MO). All other chemicals were analytical grade.

Protein Mutagenesis and Purification. Generation of recombinant CaM mutants was carried out as previously described (*10*). Mutations were verified by DNA sequence analysis. Isolation of recombinant CaM mutants was via phenyl-Sepharose chromatography as previously described (*10*). Protein concentrations were determined with the extinction coefficient at 280 nm, with molar absorbtivities for CaM mutants with F19W of 7200 M^{-1} cm^{-1}.

Ca^{2+} Affinity Determination. All static fluorescence measurements were performed on a Perkin-Elmer LS5 spectrofluoremeter at 22 °C. $[Ca^{2+}]_{free}$ was calculated as described by Robertson and Potter (*28*). K_ds were calculated by adding increasing concentrations of Ca^{2+} to 1 mL of each CaM (1 μM) in 200 mM MOPS, 90 mM KCl, and 2 mM EGTA at pH 7.0 and 22 °C to yield the indicated pCa. Tryptophan fluorescence was monitored at 335 nm with excitation at 275 nm. Each reported K_d represents an average of three to five titrations ± the standard error fit with the logistic sigmoidal function, $y = y_{min} + [(y_{max} - y_{min})/\{1 + \exp[-k(x - x_{50})]\}]$, where y_{min} and y_{max} represent the minimal and maximal tryptophan fluorescence, respectively, k is proportional to the Hill coefficient ($k = n$ ln 10, where n is the Hill coefficient), x is the logarithm of $[Ca^{2+}]_{free}$, and x_{50} is the logarithm of $[Ca^{2+}]_{free}$ producing half-maximal fluorescence, as described by George et al. (*16*).

Determination of Ca^{2+} Dissociation Kinetics. All global dissociation kinetic measurements (K_{off}) were conducted at 10 °C in an Applied Photophysics Ltd. (Leatherhead, U.K.) model SF.17 stopped-flow instrument. This apparatus had a dead time of 1.6 ms and a flow rate of 17 μL/ms. The samples were excited using a 150 W xenon arc source. The dissociation rate extraction software (by P. J. King, Applied Photophysics Ltd.) uses the nonlinear Levenberg−Marquardt algorithm. Each rate represents the concerted release of two Ca^{2+} from the N-terminal Ca^{2+}-binding sites. Each trace represents an average of five to seven traces fit with a single exponential (variance $< 5 \times 10^{-4}$). All kinetic traces were triggered at time zero, and the first 1.6 ms of premixing is shown (the apparent lag phase). Each kinetic trace was fit only after premixing was complete (after 1.6 ms). Tryptophan fluorescence dissociation kinetics were determined by mixing equal volumes (50 μL) of each CaM (4 μM) and Ca^{2+} (200 μM) in 20 mM Hepes (pH 7.0) and EGTA (10 mM) in the same buffer. Excitation was at 275 nm with emission monitored through an UV transmitting black glass filter [UG1 from Oriel (Stanford, CT)]. Quin-2 fluorescence dissociation kinetics were determined by mixing equal volumes (50 μL) of each CaM (8 μM) and Ca^{2+} (60 μM) in 20 mM Hepes (pH 7.0) and Quin-2 (150 μM) in the same buffer. Excitation was at 330 nm with emission monitored with a 510 nm broad band-pass filter (Oriel). The changes in Quin-2 fluorescence were converted into moles of Ca^{2+} dissociating from the N-terminus of CaM as previously described by Johnson et al. (*6*).

Determination of Ca^{2+} Association Kinetics. Macroscopic Ca^{2+} association rates were calculated using the relationship $K_{on} = K_{off}/K_d$, assuming that K_{off} and K_d represent the concerted release or binding events of both Ca^{2+} ions from the N-terminal Ca^{2+}-binding sites. K_{off} is due to the inability to distinguish the dissociation events of the individual ions via Quin and/or tryptophan. K_d represents the concerted binding of both Ca^{2+} ions assuming that both Ca^{2+} ions bind indistinguishably to the N-terminal Ca^{2+}-binding sites of F19W CaM, as described by Wang et al. (*10*).

RESULTS

Validation of the Use of the Phe19 Replacement with Tryptophan for Analysis of the Ca^{2+} Binding Properties of the Acid Pair Mutants. The N-terminus of CaM has no

Table 1: Summary of Ca^{2+} Binding Properties for Acid Pair Mutants[a]

F19W construct	mutant protein	site I acid pairs	site II acid pairs	F19W tryptophan N-term K_d (uM)	Hill coef	F19W tryptophan N-term off rate (s^{-1})	Quin N-term off rate (s^{-1})	F19W tryptophan N-term on rate ($\times 10^6$ M^{-1} s^{-1})
WI_0II_X	F19W/D24N	none	*X*	20.4 ± 1.5	1.2 ± 0.2	155 ± 2	156 ± 5	7.6
WI_ZII_X	F19W	*Z*	*X*	4.45 ± 0.1	1.8 ± 0.1	248 ± 15	251 ± 9	56
WI_XII_X	F19W/D24N/T28D	*X*	*X*	7.8 ± 0.4	1.7 ± 0.1	23 ± 1	23 ± 2	2.9
WI_YII_X	F19W/D24N/T26D	*Y*	*X*	6.1 ± 0.3	1.6 ± 0.1	150 ± 2	152 ± 6	25
$WI_{XY}II_X$	F19W/D24N/T26D/T28D	*X, Y*	*X*	2.8 ± 0.2	1.8 ± 0.1	42 ± 3	37 ± 2	15
$WI_{XZ}II_X$	F19W/T28D	*X, Z*	*X*	2.73 ± 0.02	2.2 ± 0.1	297 ± 8	284 ± 10	110
$WI_{YZ}II_X$	F19W/T26D	*Y, Z*	*X*	2.37 ± 0.06	2.1 ± 0.1	116 ± 10	111 ± 3	49
$WI_{XYZ}II_X$	F19W/T26D/T28D	*X, Y, Z*	*X*	2.64 ± 0.06	1.7 ± 0.1	153 ± 4	150 ± 4	58
WI_ZII_0	F19W/D64N	*Z*	none	11.2 ± 0.5	1.7 ± 0.2	595 ± 37	606 ± 24	54
WI_ZII_X	F19W	*Z*	*X*	4.45 ± 0.1	1.8 ± 0.1	248 ± 15	251 ± 9	56
WI_ZII_Y	F19W/T62D/D64N	*Z*	*Y*	14.1 ± 0.6	0.8 ± 0.1	>1000	>1000	>70
WI_ZII_Z	F19W/N60D/D64N	*Z*	*Z*	2.21 ± 0.03	2.4 ± 0.1	162 ± 1	165 ± 3	74
WI_ZII_{XY}	F19W/T62D	*Z*	*X, Y*	6.7 ± 0.2	1.6 ± 0.1	762 ± 51	829 ± 32	120
WI_ZII_{XZ}	F19W/N60D	*Z*	*X, Z*	2.68 ± 0.02	2.2 ± 0.1	391 ± 3	413 ± 18	150
WI_ZII_{YZ}	F19W/N60D/T62D/D64N	*Z*	*Y, Z*	2.28 ± 0.03	2.7 ± 0.1	584 ± 38	549 ± 51	250
WI_ZII_{XYZ}	F19W/N60D/T62D	*Z*	*X, Y, Z*	4.1 ± 0.1	2.1 ± 0.3	368 ± 14	372 ± 18	89
WI_0II_0	F19W/D24N/D64N	none	none	47.9 ± 4.6	1.0 ± 0.2	417 ± 16	405 ± 11	8.5
$WI_{XYZ}II_{XYZ}$	F19W/T26D/T28D/ N60D/T62D	*X, Y, Z*	*X, Y, Z*	26.3 ± 1.2	1.7 ± 0.2	648 ± 13	652 ± 40	25

[a] Each tryptophan K_d represents an average of three to five titrations ± the standard error. Each dissociation kinetic measurement (K_{off}) represents an average of five to seven traces fit with a single exponential (variance $< 5 \times 10^{-4}$). Tryptophan Ca^{2+} association rates were calculated using the relationship $K_{on} = K_{off}/K_d$.

intrinsic fluorescent probe to directly follow Ca^{2+} binding to these sites. To follow Ca^{2+} binding directly to the N-terminus of CaM, F19 was replaced with W, which allowed for a Ca^{2+}-dependent tryptophan fluorescence increase of approximately 3-fold (*29*). This mutation is analogous to the F29W mutation utilized to determine Ca^{2+} affinity and exchange rates within the sites of the N-terminus of sTnC that regulate skeletal muscle contraction and relaxation (*30*). Similar tryptophan mutations have allowed the determination of the order of Ca^{2+} binding to CaM (*31*). The tryptophan fluorescence dissociation rates were verified by analysis with the Ca^{2+} chelator Quin-2. Using Quin-2, we observed ~2 mol of Ca^{2+} dissociating from the N-terminus of F19W CaM at a single dissociation rate. The absolute correlation between the F19W and Quin-2 Ca^{2+} dissociation rates (Table 1) suggests that the F19W mutation in the N-terminus of CaM reports Ca^{2+} binding directly due to the intimate association between the structural changes, which occur in CaM, and the binding of Ca^{2+}. Thus, the change in W19 fluorescence is an accurate report of global Ca^{2+} binding to the N-terminus of CaM.

Ca^{2+} Binding and N-Terminal Ca^{2+} Exchange Rates in Site I Acid Pair CaM Mutants with Native Ca^{2+}-Binding Site II. We wanted to see if the acid pair hypothesis could be extended to the functional coupled EF-hand system of the N-terminal Ca^{2+}-binding sites in F19W CaM by increasing the number of acid pairs in Ca^{2+}-binding site I of CaM from zero to three. Figure 2 shows the Ca^{2+}-dependent increase in tryptophan fluorescence of $WI_{XYZ}II_X$, $WI_{YZ}II_X$, WI_ZII_X, and WI_0II_X (where W represents a CaM mutant with the Phe19Trp mutation, I and II represent the Ca^{2+}-binding loops in the first and second N-terminal EF-hands of CaM, respectively, and *X*, *Y*, and *Z* represent the acid pairs that are present in each Ca^{2+}-binding loop). Each mutant exhibited half-maximal saturation at 2.6, 2.4, 4.4, and 20.4 μM for $WI_{XYZ}II_X$, $WI_{YZ}II_X$, WI_ZII_X, and WI_0II_X, respectively (Table 1). The endogenous *Z*-axis acid pair in N-terminal Ca^{2+}-

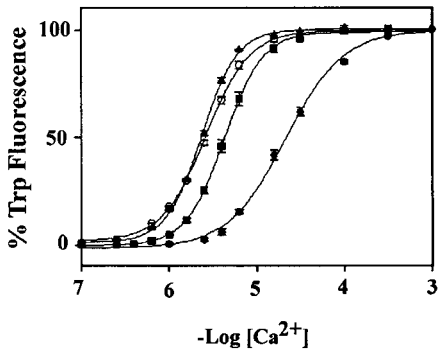

FIGURE 2: Ca^{2+} binding to site I acid pair mutants with a functional site II. This figure shows the Ca^{2+}-dependent increase in tryptophan fluorescence for $WI_{XYZ}II_X$ (▲), $WI_{YZ}II_X$ (○), WI_ZII_X (■), and WI_0II_X (●), a representative set of the site I F19W CaM mutants, as a function of $-\log[Ca^{2+}]$. Increasing concentrations of Ca^{2+} were added to 1 mL of each CaM (1 μM) in 200 mM MOPS, 90 mM KCl, and 2 mM EGTA at pH 7.0 and 22 °C to yield the indicated pCa. The pCa was determined as described in Materials and Methods. Tryptophan fluorescence was monitored at 335 nm with excitation at 275 nm. Each K_d represents an average of three to five titrations ± the standard error; 100% fluorescence corresponds to a 3.1-, 2.8-, 2.9-, and 2.8-fold increase in tryptophan fluorescence for $WI_{XYZ}II_X$, $WI_{YZ}II_X$, WI_ZII_X, and WI_0II_X, respectively.

binding site I of F19W CaM (WI_ZII_X) increases the N-terminal Ca^{2+} affinity ~4.6-fold in comparison to that of WI_0II_X. The highest N-terminal Ca^{2+} affinity (2.4 μM) occurred when there were two acid pairs in Ca^{2+}-binding site I located at the *Y*- and *Z*-axis positions ($WI_{YZ}II_X$), creating an ~8.5-fold increase in Ca^{2+} affinity relative to that of WI_0II_X. When the number of acid pairs in site I increased from zero to three, while leaving site II unmodified, nearly 65% (~5-fold) of the maximal increase in N-terminal Ca^{2+} affinity in relation to that of WI_0II_X was obtained when there was a single acid pair located at any of the axis positions, *X*, *Y*, or *Z*. Approximately 90% (8-fold) of the increase in N-terminal Ca^{2+} affinity was obtained when there were two

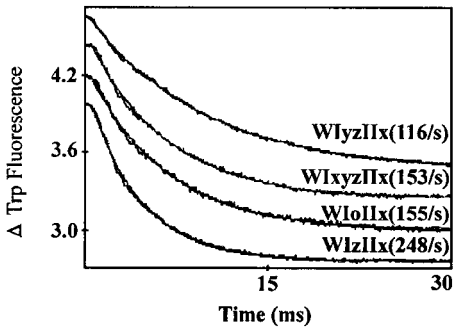

FIGURE 3: Ca^{2+} dissociation from site I acid pair mutants with a functional site II. This figure shows the decrease in tryptophan fluorescence associated with Ca^{2+} dissociation from the N-terminal sites of $WI_{XYZ}II_X$, $WI_{YZ}II_X$, WI_ZII_X, and WI_0II_X, a representative set of the site I F19W CaM mutants. Measurements were conducted by mixing equal volumes (50 μL) of each CaM (4 μM) and Ca^{2+} (200 μM) in 20 mM Hepes (pH 7.0) and EGTA (10 mM) in the same buffer at 10 °C. Excitation was at 275 nm with emission monitored through an UV transmitting black glass filter (UG1 from Oriel). Each trace represents an average of five to seven traces fit with a single exponential (variance $< 5 \times 10^{-4}$).

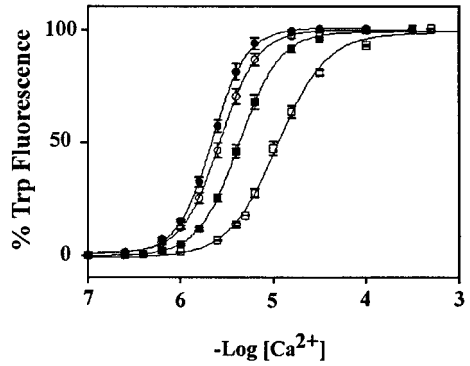

FIGURE 4: Ca^{2+} binding to site II acid pair mutants with a functional site I. This figure shows the Ca^{2+}-dependent increase in tryptophan fluorescence for WI_ZII_{XZ} (○), WI_ZII_X (■), WI_ZII_Z (●), and WI_ZII_0 (□), a representative set of the site II F19W CaM mutants, as a function of $-\log[Ca^{2+}]$. Measurements were conducted as described in the legend of Figure 2; 100% fluorescence corresponds to a 3.0-, 2.9-, 2.7-, and 3.1-fold increase in tryptophan fluorescence for WI_ZII_{XZ}, WI_ZII_X, WI_ZII_Z, and WI_ZII_0, respectively.

acid pairs located at any of the axis positions, *X*, *Y*, or *Z*. Addition of the third acid pair in site I did not significantly increase N-terminal Ca^{2+} affinity relative to the N-terminal Ca^{2+} affinity associated with having two acid pairs (Table 1). WI_0II_X had a reduced Hill coefficient of 1.2, implicating the need for an acid pair in site I for positive cooperativity between the two EF-hands in CaM's N-terminal domain. Although the addition of any axis acid pair was capable of increasing N-terminal Ca^{2+} affinity and restoring cooperativity, the largest increases in N-terminal Ca^{2+} affinity were seen with the addition of the *Z*-axis acid pair. Therefore, increasing the number of acid pairs in site I, while site II was native, increased the N-terminal Ca^{2+} affinity, with the *Z*-axis acid pair being the most significant determinant for N-terminal Ca^{2+} affinity (Figure 2 and Table 1).

Fluorescence stopped-flow measurements were utilized to evaluate the effects of increasing the number of acid pairs in site I of F19W CaM on the global rates of N-terminal Ca^{2+} dissociation (K_{off}). Figure 3 shows the rates of the EGTA-induced decrease in tryptophan fluorescence due to the concerted release of both Ca^{2+} ions from N-terminal Ca^{2+}-binding site I mutants. Ca^{2+} dissociated from the N-termini of $WI_{XYZ}II_X$, $WI_{YZ}II_X$, WI_ZII_X, and WI_0II_X at rates of 153, 116, 250, and 155 s^{-1}, respectively. The Ca^{2+} dissociation rates reported by the tryptophan fluorescence suggest that there was no universal correlation between a decrease in Ca^{2+} dissociation rates and the increases observed in N-terminal Ca^{2+} affinity associated with an increase in the number of acid pairs in Ca^{2+}-binding site I (Figure 3 and Table 1). Only the *X*-axis acid pair mutants invariably showed a correlation with their observed increases in N-terminal Ca^{2+} affinity and decreases in their N-terminal Ca^{2+} dissociation rates in comparison to F19W CaMs without an *X*-axis acid pair. We then calculated the global Ca^{2+} association rates (K_{on}) for these mutants using the relationship $K_{on} = K_{off}/K_d$, as described by Wang et al. (*10*). These calculations are shown in Table 1 (tryptophan N-term on rate). Usually, as an acid pair was added, the Ca^{2+} association rate increased (Table 1). Thus, the increase in N-terminal Ca^{2+} affinity associated with increasing the number of acid pairs in site I, while site II was native, was due to alterations in the Ca^{2+} association rates whose magnitudes were greater than the magnitudes of the changes seen in the Ca^{2+} dissociation rates in relation to the mutant without an acid pair in site I (WI_0II_X).

Ca^{2+} Binding and N-Terminal Ca^{2+} Exchange Rates in Site II Acid Pair CaM Mutants with Native Ca^{2+}-Binding Site I. Figure 4 shows the Ca^{2+}-dependent increases in tryptophan fluorescence of WI_ZII_{XZ}, WI_ZII_Z, WI_ZII_X, and WI_ZII_0. Each mutant exhibited half-maximal saturation at 2.7, 2.2, 4.4, and 11.2 μM for WI_ZII_{XZ}, WI_ZII_Z, WI_ZII_X, and WI_ZII_0, respectively (Table 1). The endogenous *X*-axis acid pair in N-terminal Ca^{2+}-binding site II of F19W CaM (WI_ZII_X) increased N-terminal Ca^{2+} affinity ~2.5-fold compared to that of WI_ZII_0. The highest N-terminal Ca^{2+} affinity (2.2 μM) occurred when there was only one acid pair in Ca^{2+}-binding site II located on the *Z*-axis (WI_ZII_Z), creating an ~5-fold increase in Ca^{2+} affinity in relation to that of WI_ZII_0. Upon addition of an *X*-axis acid pair in site II with site I remaining native, Ca^{2+} affinity increased ~2.5-fold in comparison to that of WI_ZII_0, with further increases in N-terminal Ca^{2+} affinity observed only with the addition of a *Z*-axis acid pair. Addition of the *Y*-axis acid pair in site II decreased N-terminal Ca^{2+} affinity and reduced the Hill coefficient when site I was unmodified in comparison to the F19W CaM that did not contain the *Y*-axis acid pair. Thus, the *X*- and *Z*-axis acid pairs increased the N-terminal Ca^{2+} affinity in site II when site I was unmodified with the *Z*-axis acid pair being the most significant determinant, as was seen in site I.

Fluorescence stopped-flow measurements were utilized to evaluate the effects of increasing the number of acid pairs in site II of F19W CaM on the global rates of N-terminal Ca^{2+} dissociation (K_{off}). Figure 5 shows the rates of the EGTA-induced decrease in tryptophan fluorescence due to the concerted release of both Ca^{2+} ions from N-terminal Ca^{2+}-binding site II mutants. Ca^{2+} dissociated from the N-termini of WI_ZII_{XZ}, WI_ZII_X, WI_ZII_Z, and WI_ZII_0 at rates of 391, 250, 162, and 595 s^{-1}, respectively. The Ca^{2+} dissociation rates reported by the tryptophan fluorescence again indicate a correlation between the decreases in the Ca^{2+} dissociation rates and the increases observed in N-terminal Ca^{2+} affinity for the *X*-axis acid pair mutants (Table 1). For

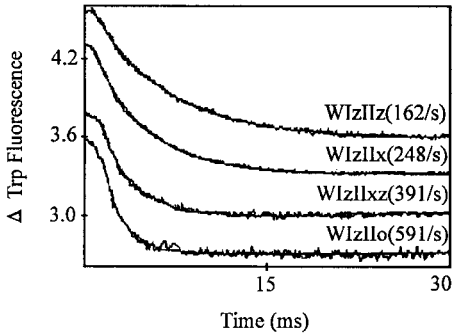

FIGURE 5: Ca^{2+} dissociation from site II acid pair mutants with a functional site I. This figure shows the decrease in tryptophan fluorescence associated with Ca^{2+} dissociation from the N-terminal sites of WI_ZII_{XZ}, WI_ZII_X, WI_ZII_Z, and WI_ZII_0, a representative set of the site II F19W CaM mutants. Measurements were conducted as described in the legend of Figure 3.

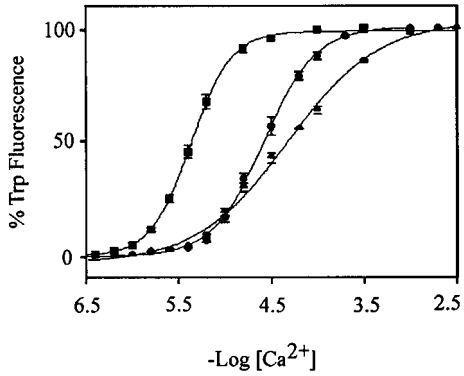

FIGURE 6: Ca^{2+} binding to N-terminal Ca^{2+}-binding site I and site II acid pair mutants. This figure shows the Ca^{2+}-dependent increase in tryptophan fluorescence for $WI_{XYZ}II_{XYZ}$ (■), WI_ZII_X (●), and WI_0II_0 (▲), as a function of $-\log[Ca^{2+}]$. Measurements were conducted as described in the legend of Figure 2; 100% fluorescence corresponds to a 3.1-, 2.9-, and 2.8-fold increase in tryptophan fluorescence for $WI_{XYZ}II_{XYZ}$, WI_ZII_X, and WI_0II_0, respectively.

example, in WI_ZII_X, the N-terminal Ca^{2+} affinity increased approximately 2.5-fold relative to the N-terminal Ca^{2+} affinity of WI_ZII_0, while its N-terminal Ca^{2+} dissociation rate decreased ~2.3-fold. We again calculated the global Ca^{2+} association rates for these mutants (Table 1). As in site I, as an acid pair was added to Ca^{2+}-binding site II, the Ca^{2+} association rates were modified to a greater extent than the Ca^{2+} dissociation rates in relation to the site II mutant without an acid pair (WI_ZII_0). Thus, in site II of F19WCaM, while site I was native, the increases in the Ca^{2+} association rate due to the acid pairs primarily caused the observed increases in N-terminal Ca^{2+} affinity.

Ca^{2+} Binding and N-Terminal Ca^{2+} Exchange Rates in Site I and Site II Acid Pair CaM Mutants. To fully evaluate the acid pair hypothesis, we created F19W CaMs with no acid pairs or with all of the acid pairs filled. Figure 6 shows the Ca^{2+}-dependent tryptophan fluorescence increase of $WI_{XYZ}II_{XYZ}$, WI_ZII_X, and WI_0II_0. Each mutant exhibited half-maximal saturation at 26.4, 4.4, and 47.9 μM for $WI_{XYZ}II_{XYZ}$, WI_ZII_X, and WI_0II_0, respectively (Table 1). The endogenous acid pairs in the N-terminal Ca^{2+}-binding sites of F19W CaM are responsible for an ~11-fold increase in N-terminal Ca^{2+} affinity relative to the N-terminal Ca^{2+} affinity of WI_0II_0. Having acid pairs at each axis position in the N-terminal Ca^{2+}-binding sites ($WI_{XYZ}II_{XYZ}$) increased the N-terminal Ca^{2+} affinity only ~2-fold in comparison to the N-terminal Ca^{2+} affinity of WI_0II_0. As was seen in site I, when there were no acid pairs present in either EF-hand, the Hill coefficient was significantly reduced. Hence, as was seen in sites I and II, increasing the number of acid pairs within the EF-hand Ca^{2+}-binding loops increased N-terminal Ca^{2+} affinity.

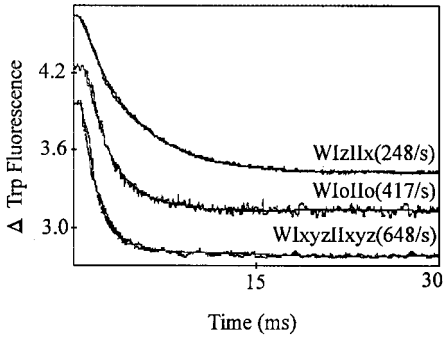

FIGURE 7: Ca^{2+} dissociation from N-terminal Ca^{2+}-binding site I and site II acid pair mutants. This figure shows the decrease in tryptophan fluorescence associated with Ca^{2+} dissociation from the N-terminal sites of $WI_{XYZ}II_{XYZ}$, WI_ZII_X, and WI_0II_0. Measurements were conducted as described in the legend of Figure 3.

Fluorescence stopped-flow measurements were utilized to evaluate the effects of altering the number of acid pairs in N-terminal Ca^{2+}-binding sites of F19W CaM on the global rates of N-terminal Ca^{2+} dissociation (K_{off}). Figure 7 shows the rates of EGTA-induced decrease in tryptophan fluorescence due to the concerted release of both Ca^{2+} ions from the N-terminal Ca^{2+}-binding site mutants. Ca^{2+} dissociated from the N-termini of $WI_{XYZ}II_{XYZ}$, WI_ZII_X, and WI_0II_0 at rates of 648, 250, and 417 s^{-1}, respectively. We again calculated the global Ca^{2+} association rates for these mutants (Table 1). As was seen with earlier mutants, the gains in N-terminal Ca^{2+} affinity were primarily due to greater alterations in the Ca^{2+} association rates versus the observed changes in the Ca^{2+} dissociation rates in relation to the mutant containing no acid pairs (WI_0II_0).

DISCUSSION

This paper focuses on testing the acid pair hypothesis in a functional, coupled EF-hand protein system. We generated a series of CaM mutants with the number of acid pairs increasing from zero to three in the N-terminal Ca^{2+}-binding sites to obtain a relationship between the number and location of acid pairs in a functional coupled EF-hand protein system. When we increased the number of acid pairs in CaM's N-terminal Ca^{2+} binding sites, the N-terminal Ca^{2+} affinity increased in relation to the respective mutants which contained no acid pairs. Accordingly, the general rule of the acid pair hypothesis, that additional acid pairs within the Ca^{2+} binding loops of an EF-hand increase Ca^{2+} affinity, has been confirmed.

Each two-acid pair mutant had five chelating acids within the Ca^{2+}-binding loop; only the site II mutant containing an *X*- and *Y*-axis acid pair displayed a decrease in the N-terminal Ca^{2+} affinity observed in relation to the maximal observed Ca^{2+} affinity in CaM containing four acidic chelating residues. For the remaining mutants containing five acidic chelating residues, each had a higher or similar N-terminal Ca^{2+} affinity in comparison to those of their respective site mutants containing only four acidic chelating residues. These results are directly opposed to the acid pair hypothesis, which

predicted a loss in affinity because of the presence of a fifth acidic chelating residue due to electrostatic repulsion. However, these results are consistent with observations from structure−function studies in oncomodulin which raised its Ca^{2+} affinity by introducing a fifth acidic chelating residue within the Ca^{2+}-binding loop (*22*). Only when each Ca^{2+}-binding site had a full complement of acid pairs was there a significant reduction in the N-terminal Ca^{2+} affinity. Presumably, this is due to local perturbations distorting the loop conformation needed for high-affinity Ca^{2+} binding because of electrostatic repulsion within or between the two EF-hands.

In this study, three mutants (WI_0II_X, WI_ZII_Y, and WI_0II_0) had Hill coefficients of ≤ 1.2, indicating a lack of cooperativity between the two N-terminal EF-hands. Each of these mutants also had low N-terminal Ca^{2+} affinities. Mutants with Hill coefficients, indicating full cooperativity, did not experience a decrease in Ca^{2+} affinity, even though many had five acidic chelating residues. This indicates that cooperativity between the two N-terminal EF-hands is essential for high-affinity Ca^{2+} binding. The cooperativity between the two N-terminal EF-hands may also account for the discrepancies between the observed and predicted results due to the acid pair hypothesis for mutants containing five acidic chelating residues.

Calculation of the global Ca^{2+} association rates ($K_{on} = K_{off}/K_d$) demonstrated that the increases observed in N-terminal Ca^{2+} affinity were primarily associated with increases in the rates of Ca^{2+} association. This was surprising in the case of the *Y*-axis acid pair, since interaction with Ca^{2+} at the $-y$ position is through the backbone carbonyl and not the side chain residue. In the site I mutants, this increase in the Ca^{2+} association rate correlated to an increase in the N-terminal Ca^{2+} affinity. Most likely, this is due to stabilization of the Ca^{2+}-bound state. The $-y$ position in site I of CaM has greater solvent accessibility (solvent accessible surface calculation) in the Ca^{2+}-bound state than it has in the apo state [based on crystal and NMR structures (*32*, *37*)]; thus, an acidic residue at this position should stabilize the Ca^{2+}-bound state. This is supported by hydrophobic core substitutions in calbindin D_{9k} that caused a destabilization of the apoprotein and a stabilization of the Ca^{2+}-loaded protein associated with an increase in Ca^{2+} affinity (*38*). Alternatively, the $-y$ position in site II has a decrease in solvent accessibility upon binding of the Ca^{2+}; thus, an acidic residue at this position should stabilize the apo state. This would account for the increased Ca^{2+} dissociation rate leading to a reduction in Ca^{2+} affinity for the site II *Y*-axis acid pair mutant.

The increases in affinity due to the addition of the *Z*-axis acid pair are not surprising since the *Z*-axis acid pair helps to define the planar pentagonal arrangement utilized by EF-hands in the binding of Ca^{2+} (*14*) and has previously been demonstrated to be a significant determinant for Ca^{2+} affinity and binding (*27*). Presumably, the presence of the *Z*-axis acid pair increased the Ca^{2+} association rates by increasing the electrostatic attraction for Ca^{2+} within the coordination sphere due to the presence of the carboxylate group of the residue side chain. Addition of the *X*-axis acid pair increased the N-terminal Ca^{2+} affinity due to reduction of the Ca^{2+} dissociation rate, not an increase in the Ca^{2+} association rate. This is consistent with the gateway hypothesis in which an EF-hand which contains a negatively charged residue at the $-x$ position of the Ca^{2+}-binding loop should have a slower Ca^{2+} dissociation rate than a Ca^{2+}-binding loop containing a neutral residue at the $-x$ position due to electrostatic interactions (*36*, *37*). Even though the *X*-axis acid pair invariably slowed the Ca^{2+} dissociation by itself, mutants containing combinations of acid pairs, including the *X*-axis acid pair, experienced an increase in their Ca^{2+} association rates, indicating that the main contribution to the increases observed in N-terminal Ca^{2+} affinity is due to increasing the Ca^{2+} association rate with the addition of an acid pair(s).

Since the majority of the acid pair mutants in this study that experienced an increase in N-terminal Ca^{2+} affinity also experienced an increase in the Ca^{2+} association rates, it is possible that the role of the acid pairs within an EF-hand is to increase the Ca^{2+} association rate. The acid pairs should increase the Ca^{2+} association rates by aiding in the desolvation of Ca^{2+} due to direct side chain chelation, previously suggested by Linse and Forsen (*39*). The acid pairs may also increase the Ca^{2+} association rates due to an increase in the electrostatic attraction for the ion. The same relationship exists for calbindin D_{9k}; reducing the number of charges near the Ca^{2+}-binding loop decreased the Ca^{2+} association rates (*40*).

Thus, in the functional paired EF-hand system of the N-terminus of CaM, we have shown that increasing the number of acid pairs in the N-terminal Ca^{2+}-binding sites of CaM increased the Ca^{2+} affinities for these mutants. The maximum increases in Ca^{2+} affinity for site I require acid pairs at any axis position (*X*, *Y*, or *Z*), while maximal increases in Ca^{2+} affinity for site II required a *Z*-axis acid pair. Additionally, completely filling the acid pairs within the N-terminal Ca^{2+}-binding sites of CaM is detrimental to high-affinity Ca^{2+} binding. Furthermore, the increases in Ca^{2+} affinities with an increasing number of acid pairs were shown to be primarily due to an increase in the ion association rates.

ACKNOWLEDGMENT

We appreciate the critical reading of the manuscript by Dr. Ruth A. Altschuld, Dr. Charles L. Brooks, and Dr. Anthony R. Means.

REFERENCES

1. Van Eldik, L. J., and Watterson, D. M., Eds. (1998) *Calmodulin and Signal Transduction*, Academic Press, New York.
2. Martin, S. R., Teleman, A. A., Bayley, P. M., Drakenberg, T., and Forsen, S. (1985) *Eur. J. Biochem. 151*, 543−550.
3. Suko, J., Pidlich, J., and Bertel, O. (1985) *Eur. J. Biochem. 153*, 451−457.
4. Suko, J., Wyskovsky, W., Pidlich, J., Hauptner, R., Plank, B., and Hellmann, G. (1986) *Eur. J. Biochem. 159*, 425−434.
5. Linse, S., Helmersson, A., and Forsen, S. (1991) *J. Biol. Chem. 266*, 8050−8054.
6. Johnson, J. D., Snyder, C., Walsh, M., and Flynn, M. (1996) *J. Biol. Chem. 271*, 761−767.
7. Linse, S., Jonsson, B., and Chazin, W. J. (1995) *Proc. Natl. Acad. Sci. U.S.A. 92*, 4748−4752.
8. Maune, J. F., Klee, C. B., and Beckingham, K. (1992) *J. Biol. Chem. 267*, 5286−5295.
9. Wu, X., and Reid, R. E. (1997) *Biochemistry 36*, 8649−8656.
10. Wang, S., George, S. E., Davis, J. P., and Johnson, J. D. (1998) *Biochemistry 37*, 14539−14544.
11. Kretsinger, R. H., and Nockolds, C. E. (1973) *J. Biol. Chem. 248*, 3313−3326.

12. Marsden, B. J., Shaw, G. S., and Sykes, B. D. (1990) *Biochem. Cell Biol. 68*, 587−601.
13. Falke, J. J., Drake, S. K., Hazard, A. L., and Peersen, O. B. (1994) *Q. Rev. Biophys. 27*, 219−290.
14. Strynadka, N. C. J., and James, M. N. G. (1989) *Annu. Rev. Biochem. 58*, 951−988.
15. Trigo-Gonzalez, G., Awang, G., Racher, K., Neden, K., and Borgford, T. (1993) *Biochemistry 32*, 9826−9831.
16. George, S. E., Su, Z., Fan, D., Wang, S., and Johnson, J. D. (1996) *Biochemistry 35*, 8307−8313.
17. Browne, J. P., Strom, M., Martin, S. R., and Bayley, P. M. (1997) *Biochemistry 36*, 9550−9561.
18. Shama, Y., Chandani, S., Sukhaswami, M. B., Uma, L., Balasubramanian, D., and Fairwell, T. (1997) *Eur. J. Biochem. 243*, 42−48.
19. Potter, J. D., Johnson, J. D., Dedman, J. R., Schreiber, W. E., Mandel, F., Jackson, R. L., and Means, A. R. (1977) in *Calcium Binding Proteins and Calcium Function* (Wasserman, R. H., et al., Eds.) pp 239−250, Elsevier North-Holland Inc., New York.
20. Babu, A., Su, H., and Gulati, J. (1993) in *Mechanism of Myofilament Sliding in Muscle Contraction* (Sugi, H., and Pollack, G. H., Eds.) pp 125−131, Plenum Press, New York.
21. Waltersson, Y., Linse, S., Brodin, P., and Grundstrom, T. (1993) *Biochemistry 32*, 7866−7871.
22. Henzl, M. T., Hapak, R. C., and Goodpasture, E. A. (1996) *Biochemistry 35*, 5856−5869.
23. Henzl, M. T., Hapak, R. C., and Likos, J. J. (1998) *Biochemistry 37*, 9101−9111.
24. Reid, R. E., and Hodges, R. S. (1980) *J. Theor. Biol. 84*, 401−444.
25. Marsden, B. J., Hodges, R. S., and Sykes, B. D. (1988) *Biochemistry 27*, 4198−4206.
26. Reid, R. E. (1990) *J. Biol. Chem. 265*, 5971−5976.
27. Procyshyn, R. M., and Reid, R. E. (1994) *J. Biol. Chem. 269*, 1641−1647.
28. Robertson, S., and Potter, J. D. (1984) *Methods Pharmacol. 5*, 63−75.
29. Johnson, J. D., and Tikunova, S. B. (2000) *Methods in Molecular Biology: Calcium-binding proteins protocols*, Humana Press, Totowa, NJ (in press).
30. Johnson, J. D., Nakkula, R. J., Vasulka, C., and Smillie, L. B. (1994) *J. Biol. Chem. 269*, 8919−8923.
31. Kilhoffer, M., Kubina, M., Travers, F., and Haiech, J. (1992) *Biochemistry 31*, 8098−8106.
32. Chattopadhyaya, R., Meador, W., Means, A., and Quiocho, F. (1992) *J. Mol. Biol. 228*, 1177−1192.
33. Slupsky, C. M., and Sykes, B. D. (1995) *Biochemistry 34*, 15953−15964.
34. Houdusse, A., and Cohen, C. (1996) *Structure 4*, 21−32.
35. Reid, R. E. (1987) *Biochemistry 26*, 6070.
36. Renner, M., Danielson, M. A., and Falke, J. J. (1993) *Proc. Natl. Acad. Sci. U.S.A. 90*, 6493−6497.
37. Drake, S. K., and Falke, J. J. (1996) *Biochemistry 35*, 1753−1760.
38. Kragelund, B. B., Jonsson, M., Bifulco, G., Chazin, W. J., Nilsson, H., Finn, B. E., and Linse, S. (1998) *Biochemistry 37*, 8926−8937.
39. Linse, S., and Forsen, S. (1995) *Adv. Second Messenger Phosphoprotein Res. 30*, 89−151.
40. Martin, S. R., Linse, S., Johansson, C., Bayley, P. M., and Forsen, S. (1990) *Biochemistry 29*, 4188−4193.

BI001106+